Description, Origination and Prediction of Geomagnetic Storm

Zongyuan Ge *

Department of Information Science and Engineering, Ocean University of China, Qingdao, China

* Corresponding author: 22020011011@stu.ouc.edu.cn

Abstract. The research of geomagnetic storm has developed rapidly, and many new geomagnetic storm prediction methods have appeared. In order to summarize the previous research on geomagnetic storms, and points out the improvement direction of several existing forecasting methods. This paper uses the method of literature research to introduce the basic knowledge of geomagnetic storms, the interplanetary origin, and three forecasting methods: analysis of the change of cosmic ray flux to predict geomagnetic storms, evaluation of neural networks to analyze solar wind data for geomagnetic storm prediction and using very low frequency signal to predict geomagnetic storms. The advantages and disadvantages of the above three forecasting methods are compared. According to the analysis, one can have a relatively comprehensive understanding of geomagnetic storms and grasp the basic ideas of the existing geomagnetic storm forecast methods, the forecast lead and accuracy of geomagnetic storm can be achieved by combining many existing forecasting methods. A deeper study of the relationship between Earth and the Sun could also lead to the discovery of new methods for predicting geomagnetic storms.

Keywords: geomagnetic storm, origination, prediction.

1. Introduction

The atmospheric changes often mentioned in human daily life refer to the meteorological differences of the air such as cloudy, sunny, rain and snow, and the distance space range within 30km from the earth. The space environment conditions are very different from the weather in daily life, which refers to the entire solar-earth space, magnetosphere, ionosphere, thermosphere, solar surface, and solar wind from the Earth's upper atmosphere above 30 kilometers to the sun's immediate or transient circumstances. Scientific studies have found that the space range of more than 30km is closely related to human aerospace and military activities, so the space weather directly affects the performance of ground and space equipment and people's lives.

The sun is the solar system in the mass of the largest, the hottest star, atmospheric pressure is more than four hundred billion times the Earth. The sun continues to emit huge energy to the outside space. However, while the sun provides energy to human beings, it also has some negative effects, such as ultraviolet damage to the skin when the sun is active. Especially when the sunspot activity is relatively strong, the number of flares erupting from the sun's surface increases, and the sun's surface will radiate a large number of X-rays, ultraviolet rays, high-energy particles, and so on. Among them, the current formed by high-energy particles protons and electrons, which is called the solar wind, impacts the Earth at a speed of about 300km/s, altering the ionosphere and having an impact on the Earth's magnetic field, which will cause a change in direction, which is known as geomagnetic storms.

Geomagnetic storms are simply called magnetic storms. When the magnetosphere is subjected to a sufficiently powerful and persistent interplanetary convective electric field, through strong excitation of the magnetosphere-ionospheric system, the ring current is greatly increased, sufficient to surpass the Dst index's limit index when a certain amount of geomagnetic storm occurs, and a magnetic storm is said to have occurred [1]. The X-rays, ultraviolet light, visible light and high-energy protons and electrons emitted by the flare will cause a violent disturbance in the Earth's magnetosphere lasting from ten to tens of hours, with a disturbance amplitude between tens of nT and hundreds of nT. During geomagnetic storms, the ionosphere, upper atmosphere and high-energy particle environment will have a strong response, and the magnetic storm will have a direct impact on the attitude control of the spacecraft. The subsequent violent disturbance of the geomagnetic field will lead to a rapid increase in the resistance of the upper atmosphere in the low Earth orbit, the

charging effect caused by the settlement of high-energy particles into the low Earth orbit, and the communication interruption caused by the ionospheric disturbance. It poses a great threat to the safe operation of spacecraft, for example: on February 3, 2022, the United States Space X Space Exploration Technology company launched 49 "star link" satellites to low Earth orbit, and the satellites successfully entered the orbit of 210 kilometers perigee and 340 kilometers apogee. However, the satellite experienced a geomagnetic storm on February 4, which resulted in a 13% increase in atmospheric density at 210 km, and a 40% increase in the average atmospheric density experienced by the two subsatellites over a 3-hour period. Faced with a sudden rise in atmospheric drag, SpaceX ordered the satellite into safe mode to minimize drag effects, but the strategy did not work. In the end, only 11 smoothly ascended into the working orbit, and the remaining 38 fell into the atmosphere and burned up, and the violent fluctuations of the geomagnetic field itself will also cause harm to a wide range of power transmission facilities and oil pipelines operating in high latitudes. For example, in 1989, a magnetic storm made the power grid in Quebec, Canada, overloaded, resulting in a wide range of power outages in the region. It lasted 9-12 hours. Therefore, geomagnetic storm forecasting is highly valued in all countries.

At present, space environment forecasting methods mainly include empirical method, statistical method and physical forecasting method. The empirical prediction posits that forecasters possess the ability to anticipate the future conditions of the space environment or the likelihood of specific space environment occurrences based on the alterations in the space environment that have been compiled from observations made by individuals. Although it has some subjective color, the empirical forecast is still one of the main methods of space environment forecast. Especially for the events with certain rules and periodic recurrence characteristics, the accuracy rate can reach more than 70%. Statistical forecasting method is based on statistical analysis method. It is one of the commonly used forecasting methods for space environment to find out the statistical law or relationship between space environment phenomena from a large number of historical data of space environment by using probability statistical theory and regression analysis, discriminant analysis, cluster analysis, time series analysis, spectrum analysis, wavelet analysis and other analysis techniques. Physical prediction focuses on understanding the physical processes and mechanisms that cause changes in the space environment, finding out the physical reasons for their occurrence, and describing them in the form of physical equations and their solutions. Therefore, this is the fundamental way to solve the problem of space environment prediction. Theoretically, the prediction accuracy should be quite high. The disadvantage of this method is that it is limited by the complexity of objective phenomena and the limitation of human cognitive ability, and the physical model of each link is usually an approximation of the actual physical process in a certain area under certain simplified conditions. In recent years, artificial intelligence (AI) methods are more widely used in space environment forecasting systems, including expert systems and artificial neural networks. The forecast expert system is a computer artificial intelligence system based on the forecast knowledge of the forecast experts, which simulates the forecast ideas and strategies of the space environment experts and solves the problem of space environment forecast. Artificial neural network is a network system which is widely interconnected through a large number of processing units (neurons). It is a simplification, abstraction and simulation of the mechanism of processing, storing and processing information with a mathematical model.

In recent years, the prediction of geomagnetic storms has also been vigorously developed. Based on different research methods, a variety of methods for predicting geomagnetic storms with high feasibility and different advantages have emerged. This paper aims to give readers a comprehensive understanding of geomagnetic storms, introduce the basic concepts and interplanetary origin of geomagnetic storms in detail, and introduce three verified methods for predicting geomagnetic storms. They are using the varying flux of cosmic rays to predict geomagnetic storms [2] and using neural networks to analyze solar wind data for geomagnetic storms prediction [3], and the use of very low frequency signals to forecast geomagnetic storms [4], and the advantages and future development of these three methods are summarized. At the end of the paper, the work of geomagnetic storm research is summarized and prospected.

2. Descriptions of Geomagnetic Storm

A geomagnetic storm refers to an intense disruption that transpires within the Earth's magnetosphere, persisting for a duration exceeding 10 to several tens of hours, the main feature is that in most parts of the Earth, the horizontal component of the magnetic field significantly decreases and then gradually recovers. The four commonly used indices are Kp, ap, AE, and Dst. Gredon and Rostoker summarized the origins and status of each of these indices in 1972. The definition of Dst solely pertains to the strength of the ring current, hence indicating the magnitude of magnetic storm activity [5]. In the field of scientific research, people use dst index to describe the intensity of geomagnetic activity.

In 1964, Sugiura proposed to select four geomagnetic stations with relatively uniform distribution near the equator and far away from the equatorial electric jet in the ionosphere E region, average the horizontal component measurement data per hour, take the difference between it and the time mean of the magnetic static day, in nats (nT), called the Dst index, and propose to use it to measure the intensity of magnetic storms. According to the different peaks of the Dst index, magnetic storms can be divided into the following four categories: Dst≤-200nT for super geomagnetic storms, -200nT<Dst≤-100nT for strong geomagnetic storms, -100nT<Dst≤-50nT for moderate geomagnetic storms, and -50nT<Dst≤-30nT for weak geomagnetic storms. Geomagnetic storms are characterized by significant fluctuations in the geomagnetic horizontal component, denoted as H. These disturbances typically exhibit amplitudes ranging from tens to hundreds of nanoteslas. Most of the morphological and statistical characteristics of magnetic storms are based on the variation of the H component in the middle and low latitudes. Geomagnetic storms fall into three stages of development as shown in Fig. 1 [6].

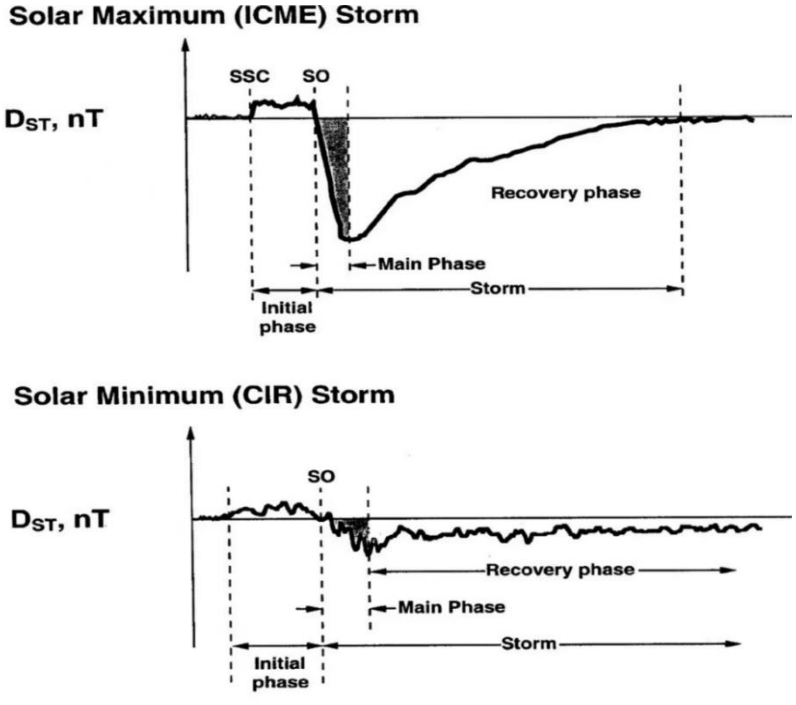


Figure 1. Magnetic storms generated by ICMEs and by CIRs

Following the onset of a magnetic storm, the horizontal component of the geomagnetic field exhibits fluctuations above the pre-storm baseline over different longitudinal locations worldwide. This phenomenon, known as the "initial phase," persists for durations ranging from tens of minutes to several hours. After the initial phase, the horizontal component soon drops to the minimum, the decline time is about half a day, the Dst index drops 100-500nT, in extreme cases may exceed 1000nT, this is the most active period of magnetic storm performance, which is call the “main phase”. Following the main phase, the H component exhibits a slow recovery towards its pre-storm level. During this temporal interval, the magnetic field exhibits fluctuations characterized by disturbances

of varying magnitudes, but with a progressive diminishing trend in the overall strength of these disturbances. Typically, the restoration of a condition of calm, referred to as the "recovery phase," requires a duration of around 2 to 3 days.

The primary and main phases of magnetic storms are caused by different physical mechanisms, the former is affected by solar wind dynamic pressure, the latter is the result of interplanetary magnetic field and Earth magnetic field reconnection, and there may be no main phase behind the primary phase. Some magnetic storms have a sudden increase in the H component at the beginning of the initial phase, which is called a sudden onset magnetic storm. Richardson and Zhang analyzed more than 1200 geomagnetic storms, in their study, it was observed that 67% of violent storms with a Dst value of 100nT or below had a two-step pattern of development. This pattern was distinguished by a subsequent decline in Dst, typically of greater magnitude. In contrast, only 29% of the storms shown a simpler, one-step rise in Dst. Surprisingly, a mere 4% of the data could not be categorized as either one-step or two-step. The suggestion put out is that the combination of two moderate storms can result in the formation of a more severe storm. It is hypothesized that when two southward components of the Interplanetary Magnetic Field (IMF) with identical timing enter the magnetosphere consecutively, this sequence triggers the consecutive occurrence of two relatively weak magnetic storms. It is suggested that the strong magnetic storm may be mainly caused by the superposition of two adjacent moderate magnetic storms [7].

According to how Dst reaches the peak through the main phase, Kamide classified geomagnetic storms into Type 1 and Type 2 categories as shown in Fig. 2. Type 1 has just one stage of development. The magnetic field on the surface of the Earth is dramatically lowered during the main phase. On the other hand, Type 2 has two development stages. That is, a two-step decreases in Dst. A new particle injection causes the ring current to rise even higher before dropping down to its pre-storm level. The latter type must meet the following conditions at the same time. The recovery range of Dst index in the first stage is less than 0.9 times of the decline range in this stage. The time interval between the minimum Dst index of the two stages is greater than 3h [8]. In addition to the first and second order development of the main phase of magnetic storms, there are more stages of development, and in general, magnetic storms whose main phase is the second or more second order development is collectively referred to as multi-stage magnetic storms.

3. The Interplanetary Origins of Geomagnetic Storms

A common explanation is that high-speed plasma clouds ejected from the solar coronal at higher speeds than the background solar wind, carrying coronal magnetic fields that impact the Earth's magnetosphere, causing it to compress and deform. Moreover, it often carries a magnetic field that rotates north to south. The magnetotail will get a massive inflow of solar wind energy when the magnetic field interacts with the geomagnetic field to the south, causing a large number of charged particles in the magnetotail plasma sheet to be injected into the ring current, which changes the intensity of the ring current, and the changing current will produce a changing magnetic field, thus causing geomagnetic storms. The development process of geomagnetic storms is as follows. The intense magnetic fields that exist between planets can be conceptually divided into two main components: the intrinsic fields and plasma connected with the coronal ejecta, referred to as driver gas fields, and the shocked and compressed fields and plasma resulting from the collision between the high-speed stream and the slower solar wind that precedes it. [1]. Geomagnetic storms are induced by the southern component of the interplanetary magnetic field, which facilitates the injection of particles from the solar wind into the magnetosphere via the process of magnetic reconnection [9]. During periods of intense magnetic storms, the efficiency of energy transmission is around 10% as shown in Figure 2 [10].

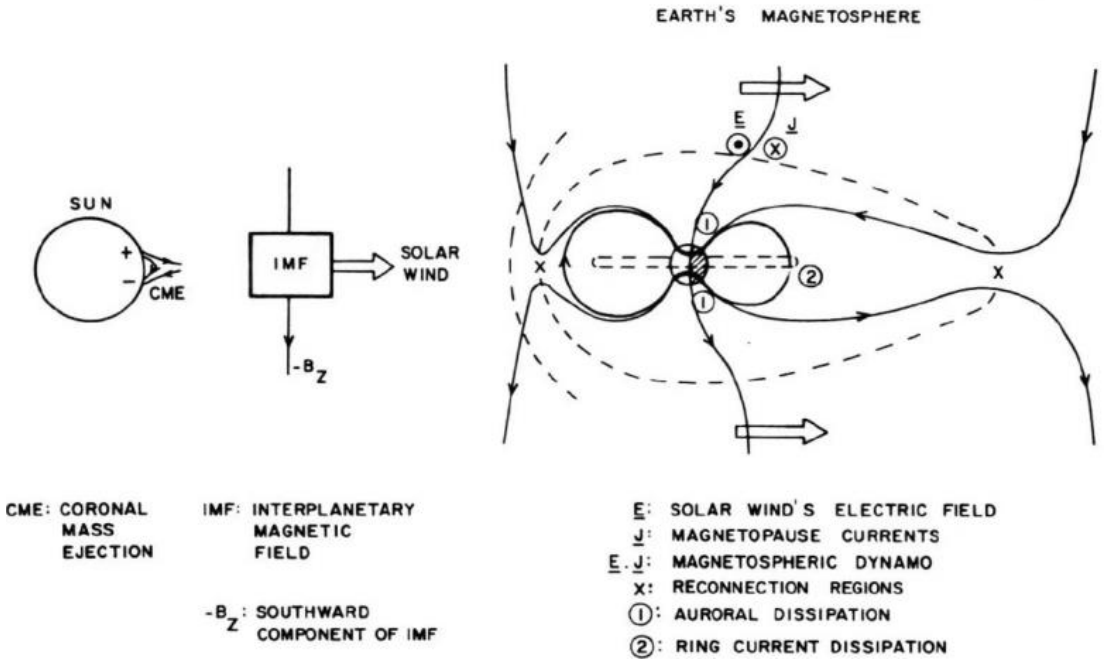


Figure 2. Interaction between the solar-interplanetary system and the magnetosphere at a period of solar maximum year

During the main phase of the magnetic storm, the ring current experiences amplification, and the injected particles coalesce to create a westward-oriented ring current. This phenomenon significantly diminishes the horizontal component of the magnetic field at the Earth's surface. With the continuous injection of particles, the ring current increases and approaches a critical value until the injection rate equals the loss rate. The recovery phase of a magnetic storm begins when the IMF weakens or rotates to the north, the ring current stops strengthening, and begins to weaken. The solar wind velocity V, plasma density ρ, the southern component of the interplanetary magnetic field Bs and its duration Δt play important roles in the development of magnetic storms. The primary factor impacting the recovery phase is the charge loss process, which encompasses charge exchange, coulomb scattering, and wave-particle interaction [11].

A lot of statistical analysis has been done on the interplanetary origin of geomagnetic storms with different intensities. The physical processes of geomagnetic perturbations caused by different types of interplanetary sources (magnetic clouds, ICME, CIR, etc.) have been described in detail in many articles, and will not be described in detail here, only the connections between different types of interplanetary sources and geomagnetic storms. During solar minimum, Earth spends 55 percent of its time in high-speed currents, 35 percent of its time in low-speed solar winds, and about 10 percent of its time in transient structures associated with CME. Geomagnetic disturbances weakened significantly during this period, with strong geomagnetic storms occurring infrequently and mostly moderate-level recurrent geomagnetic storms caused by the corotating current Interaction region (CIR). The southward component of the corotating magnetic field has strong fluctuations, so the geomagnetic storm owner is relatively weak and presents typical irregularity. During solar maximum, Earth spends only 35 percent of its time in high-speed streams, 30 percent of its time in low-speed solar winds, and about 30 percent of its time in transient structures associated with Cmes. At this time, the degree of geomagnetic disturbance increased significantly, the occurrence of large magnetic storms was more frequent, and the ICME and the sheath region behind the shock wave became the main interplanetary sources of geomagnetic storms. In particular, the compression of the forward southbound magnetic field by the shock wave, the compression of the ICME/MC by the high-speed flow, the draping of the magnetic field in front of the projectile, and multiple magnetic clouds have become the main causes of super geomagnetic storms [12].

Echer analyzed the interplanetary origin of 90 intense magnetic storms (Dst≤-100nT) occurring during the 23rd solar cycle (1996-2006). The interplanetary origin of 90 intense magnetic storms

(Dst≤-100nT) occurring during the 23rd solar cycle (1996-2006) was analyzed. 24% of the storms were caused by the magnetic clouds driving the shock wave (sMC), 24% by the sheath magnetic field (Sh),13% of these storms are caused by corotating interaction regions (CIRs), and 16% by the interaction between sheath and magnetic cloud (Sh+MC).The above four types of interplanetary sources account for three-quarters of the total number of intense magnetic storms, and another quarter are caused by magnetic cloud structures without driving shock waves (nsMC), non-magnetic cloud structures, complex structures formed by the interaction of multiple ICME, interplanetary current sheets and the interaction of Affinages in high-speed streams. They found that different interplanetary sources have different distribution characteristics in the solar cycle. sMC and Sh are the main interplanetary sources causing strong magnetic storms in the year of solar activity rising; in the year of solar activity maximum, sheath magnetic field is the main source, followed by Sh+MC and sMC, and in the year of solar activity decreasing. The main causes of severe magnetic storms are sMCSh and CIR [13]. Echer also analyzed the interplanetary origin and annual distribution of super geomagnetic storms, and found that 1/3 of the superstorms were caused by the single action of the magnetic cloud body, the interaction between the sheath and the magnetic cloud, and the single action of the magnetic field in the sheath region. Of these, 11 occurred in years of maximum solar activity (2000-2001) and six occurred in years of decreased solar activity (2003-2004) [14].

Zhang analyzed the interplanetary and solar sources of 88 intense magnetic storms (Dst≤-100nT) from 1996 to 2005 was performed, considering the relative importance of single ICME, multiple ICME, and CIR in intense magnetic storms. The findings of the study indicated that a majority of the incidents, namely 53 (60%), were attributed to a single Interplanetary Coronal Mass Ejection (ICME). Additionally, 24 (27%) incidents were found to be produced by numerous ICMEs, while 11 (13%) incidents were attributed to Corotating Interaction Regions (CIRs). The examination of the solar origins of 85 of these storms indicated that 54 (63%) were attributed to solar active areas, 11 (13%) were linked to tranquil regions connected with calm filament, 11 (13%) were related with coronal holes, and 9 (11%) were not associated with any discernible signs of explosive activity on the Sun's surface, such as the absence of flares. The absence of coronal hole darkening and other related phenomena can be attributed to the impact of coronal mass ejections (CMEs) [15]. Wu and Lepping conducted a statistical analysis to examine the correlation between 34 magnetic clouds and magnetic storms recorded during years of low solar activity (1995-1998) by using the WIND satellite observation data, and found that the magnetic field in the sheath region in front of the magnetic cloud had the same or even stronger effect than the magnetic cloud itself in the medium intensity magnetic storm [16]. In addition to the relationship between interplanetary sources and geomagnetic storms described above, Ya-Nan Tong summarized the effects of four complex interplanetary structures, namely, high-speed flow compression ICME, "interplanetary composite structure formed by multiple ejections", "multiple magnetic cloud" and "shock chasing magnetic cloud", on geomagnetic perturbations [12], which were not described in detail in this paper.

4. Prediction of geomagnetic storms

In order to improve the predictability and accuracy of geomagnetic storm prediction, a lot of work has been done. In this chapter, several geomagnetic storm prediction methods are introduced and their advantages are compared.

4.1. Change of Cosmic Ray Flux

The first method is to use the change of cosmic ray flux to predict geomagnetic storms. The physical principle is that when CME approaches the Earth, the shock wave in front of CME and the strong magnetic field carried by CME will significantly change the original orbit of cosmic ray particles, resulting in disturbance of cosmic ray flux arriving at the Earth. This disturbance is not only reflected in the change of the count of cosmic ray stations. There are also corresponding changes in the frequency signature, which can be used to predict the precursor features of geomagnetic storms.

Morlet wavelet analysis was used to analyze the cosmic ray monitoring data of cosmic ray station, the formula is as follows.

$$\Psi(t) = e^{-t^2/2} e^{j\Omega t} \tag{1}$$

The continuous record of cosmic ray flux is taken as the signal of wavelet analysis, and the continuous wavelet transform can reflect the characteristics of the time-scale transformation of the signal itself, and the overall analysis of cosmic ray flux in various frequencies is carried out. Take the wavelet analysis results of the cosmic ray flux data of Beijing Cosmic Ray Station in 2004 by Xue as an example (as illustrated in Fig. 3) [2]. The brighter the region in the figure represents the stronger the power spectrum of this location, reflecting the locality and dynamic characteristics of the time-frequency transformation of the dominant wave group of cosmic ray flux. The black thin line envelope shows the region of the wavelet influence cone, and the power spectrum outside the curve is not considered due to the boundary effect [17].

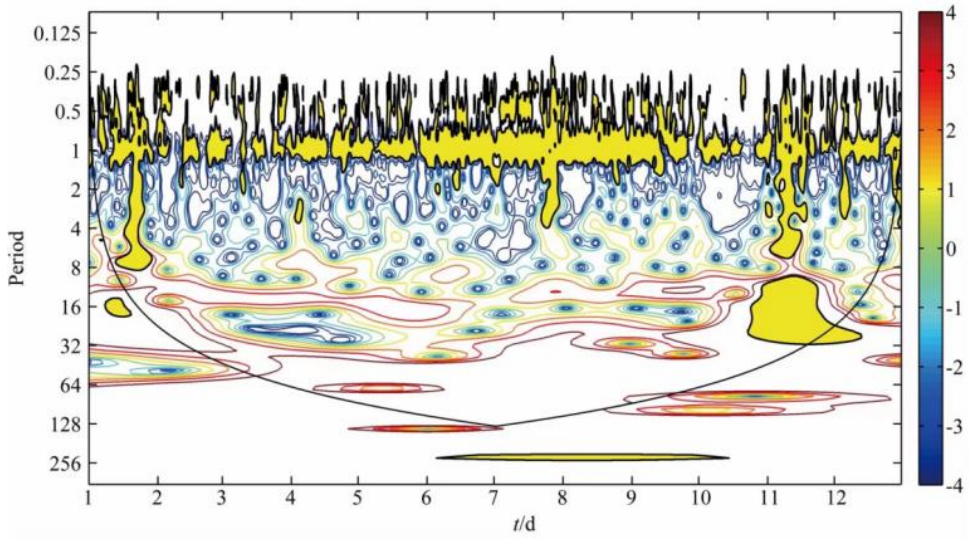


Figure 3. Morlet wavelet change of cosmic ray flux at Beijing Station in 2004.

As shown in the Fig. 3, in the quiet period, the peak value of the power spectrum of cosmic ray wavelet analysis is basically concentrated in the 12-24h period, which accords with the characteristics of quasi-24h period of cosmic ray in the quiet period. However, in late January, late July, and early November, it can be clearly seen from the images that the power spectrum is significantly enhanced in the low-frequency part except for the diurnal variation. The maximum period exceeded 16 days. By comparing with records of geomagnetic activity, geomagnetic storms occurred on January 22, July 25, and November 8, so it can be inferred that there is a relationship between the characteristics of cosmic ray flux Morlet wavelet analysis and geomagnetic storms.

Taking the geomagnetic storm on July 25 as the analysis object and taking 90d as the time window length for further refined analysis, it can be concluded that before the geomagnetic explosion, the small power spectrum had broken the original routine of 24h cycle on July 23, and the power spectrum was significantly enhanced in the low frequency part. Over the next few days, the power spectrum became more and more proportional to the long period. The above physical reason is due to the fact that in the quiet period of 24h, the wavelet frequency spectrum has a larger amplitude, and the longer period is covered up. When a magnetic storm comes, the cosmic ray disturbance makes a longer periodicity appear, and the amplitude of the corresponding long-period wavelet frequency spectrum also increases.

In order to further verify the feasibility of this prediction method, the amplitude data in Morlet wavelet analysis is extracted for further study. As illustrated in Fig. 4 [2], the amplitude of the wavelet frequency larger than 48h period changes significantly before and after geomagnetic storms, but if it

is used as a precursor before geomagnetic bursts, its prediction is insufficient. The part with a period of less than 24 hours, although there are more periods of intensification, but the amplitude increases before the arrival of strong geomagnetic storms increased more than the part with a period of more than 24 hours, and it is more suitable for analysis to improve the predictability of geomagnetic storm prediction. Taking the signal with a period of 12h as an example to analyze the amplitude change of the wavelet frequency in 2004, it can be seen that the wavelet amplitude on July 25 and November 7 increased significantly when the geomagnetic storm occurred, but on January 22, the change of the geomagnetic storm's wavelet amplitude was not obvious compared with the other two times, but also had a certain change relative to the cosmic ray background. This shows that there is a strong correspondence between the 12h period of cosmic ray wavelet amplitude and geomagnetic storm. Similarly, further refined analysis of the amplitude data shows that the wave amplitude changes significantly with the approach of CME. Observe the change of geomagnetic AP index as shown in Fig. 5 [2]. Compared with Fig. 4, it can be found that it has a good agreement with the change of wavelet amplitude.

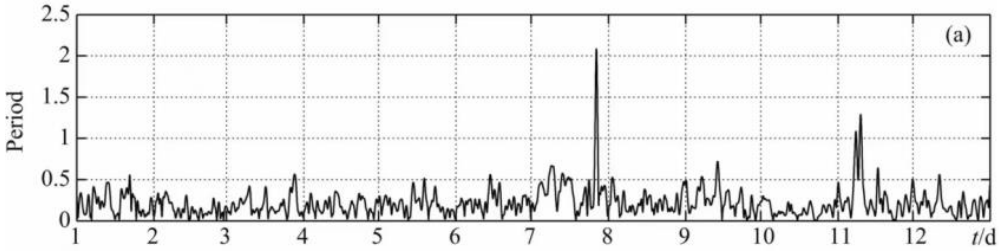


Figure 4. Amplitude changes of wavelet analysis in 2004.

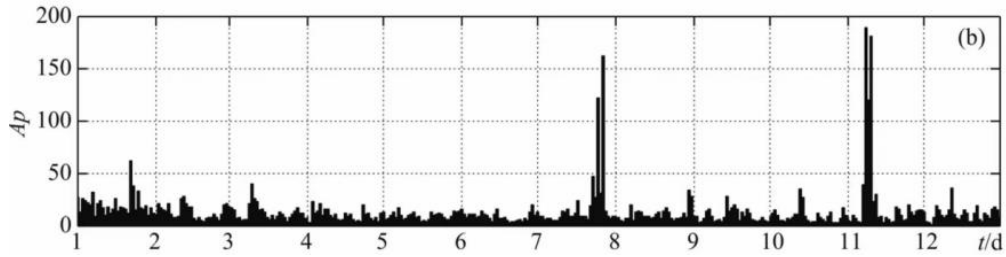


Figure 5. Changes in Ap index in 2004.

In order to further determine whether the spectrum of cosmic rays before the strong geomagnetic storm caused by CME has a similar change law, the intensity changes of 12h wave signals before all 13 strong geomagnetic storms with Kp≥7 in 2002, 2004 and 2005 are selected for progressive analysis, and it is found that the signal intensity will increase significantly and rapidly before the geomagnetic storm. Furthermore, the signal intensity 0.6 was selected as the threshold value for statistical analysis, and the threshold was used to test the prediction of 6 geomagnetic storms in 2003. The accuracy rate reached 83% [2], and the lead amount met the demand for geomagnetic storm prediction. This method can forecast the lead 1-2 days in advance while maintaining a certain accuracy. There is room for further development of the research. The above selection is the observation data of Beijing cosmic ray neutron line station. In fact, indirect information of other CME contained in cosmic ray fluctuations can be analyzed, and the fluctuation characteristics of the fixed frequency of 12h are selected as the analysis object, and the subsequent fluctuation characteristics of other frequencies can be selected as the research object to determine the frequency of the analysis object to obtain more accurate data. At the same time, the accuracy of prediction is improved by setting the appropriate threshold. In addition, the number of samples selected in the above studies is small, and more suitable methods for geomagnetic storm prediction can be obtained by selecting more samples in the future.

4.2. Neural networks to Analyze Solar Wind Data

The second method is using neural networks to analyze solar wind data for geomagnetic storm prediction. In recent years, the technology of machine learning continues to break through, and its strong parallel adaptive and self-learning information processing skills have made strides in a variety of areas. In terms of predicting geomagnetic storms, there are a variety of prediction models based on different parameters such as AE, AL, Kp and other indices. This paper only introduces the recent geomagnetic storm prediction model based on Neural Networks using Solar Wind Data. Using a sizable data set of local solar wind measurements and ground-based geomagnetic indices gathered over a 15-year period, the objective is to choose the most appropriate architecture to develop a machine learning-based predictive tool capable of effectively forecasting the future onset of any CME-induced disturbances while providing multi-hour advance warning in case critical events maprove harmful to Earth and human activities [3].

NN architectures used in this paper. The goal of the NN is to provide an early warning when the geomagnetic index SYM-H drops below 50 nT, which is the minimum acknowledged threshold for the occurrence of a geomagnetic storm. As a result, the algorithm refers to SYM-H index as the target variable. For training the NN, they collected measurements over a 15-year period from 2005 to 2019. The Internet data base OMNI [18] is used to investigate the relationship between solar wind and geomagnetic activity. Because they are most closely related to SYM-H, the data employed in OMNI are the solar wind speed U, temperature T, and density n as well as the magnetic field vector's strength B and southward-directed component Bz. To successfully train the NN, the target variable's sample must be evenly split between critical (SYM-H 50 nT) and noncritical (SYM-H> 50 nT) occurrences. To accomplish this, under sampling the noncritical class and oversampling the critical one is two augmentation procedures that have been used after data cleaning and windowing to address the imbalance of the current data [3]. This article does not go into great length on this. In the current analysis, seven alternative NNs are used to create the optimum structure for the NN including [3]:

- FNN (linear single-layer architecture, which is used as a baseline reference).
- MLP (multilayer perceptron feedforward architecture, which can improve performance).
- CNN (used on time series for predictive purposes, designed to expose spatial correlations in photos and hence uncover particular patterns in object recognition).
- LSTM (overcomes the short-term memory problem of basic recurrent designs, which stops them from propagating information from near the output back to the layers closest to the input.)
- deep CNN (an architecture created by quadrupling the size of the standard CNN model in order to improve the ability to identify relationships between input data).
- LSTM-FCN (mixes the derived outputs from several criteria to increase the NN efficiency).
- deep CNN skip (fitted with a skip connection that feeds input data into the output of the network multilayer extraction block, created to combine the ability of convolutional networks to recognize recognizable patterns in time series with the more foretelling ones offered by recurrent networks).

Table 1. Measures of performance Values of the Seven NNs Taken into Account for 1 Hour Ahead Warning of Critical Geomagnetic Events.

Network	S_C	P_C	BA	$F1_C$
CNN	0.843	0.648	0.920	0.733
Deep CNN	0.772	0.628	0.885	0.693
Linear	0.857	0.641	0.927	0.734
MLP	0.819	0.652	0.908	0.726
LSTM-FCN	0.806	0.614	0.902	0.697
LSTM	0.876	0.620	0.936	0.736
Deep CNN_{skip}	0.823	0.628	0.910	0.712

The last step of the ML process, they select the F1-score, Precision(P), Sensitivity(S), and Balanced Accuracy (BA) metrics as the assessment metrics of the performance evaluation of the proposed neural network. Defining the following: Critical event (SYM-H 50 n T) and noncritical

event (SYM-H > 50 n T) are both possible. TC and TNC (F_C and F_{NC}) are defined as the correct (incorrect), True (False) forecasts for the Critical (C) and Noncritical (NC) classes, as well as the critical class's accuracy metric. P_C, is defined as:

$$P_C = \frac{T_C}{T_C+F_C} \tag{2}$$

S_C, the percentage of accurately anticipated crucial occurrences is known as the sensitivity for the critical class, it is defined as:

$$S_C = \frac{T_C}{T_C+F_{NC}} \tag{3}$$

As sensitivity and accuracy are mutually exclusive, the harmonic mean of P_C and S_C, the F1 score is defined as:

$$F1_C = \frac{2P_CS_C}{P_C+S_C} \tag{4}$$

Sensitivity and specificity yields, expressed as an arithmetic mean, and the balanced accuracy estimate of the ML model BA as defined:

$$BA = \frac{S_C+S_{NC}}{2} = \left(\frac{T_C}{T_C+F_{NC}} + \frac{T_{NC}}{T_{NC}+F_C}\right) \tag{5}$$

The seven NN designs discussed above have been evaluated in a one-step method for forecasting severe geomagnetic disturbances 1 and 8 hour in advance. The seven NN designs outlined above were assessed in a one-step procedure for predicting severe geomagnetic disturbances one and eight hours in advance, based on the observational results obtained by Telloni et al. The metrics results of each architecture shown in the test including balanced accuracy (BA), precision (P_C), sensity (S_C) and F1 score ($F1_C$) (seen from Table. 1 and Table. 2) [3].

Table 2. Only the Five Most Efficient Architectures, Forecast 8 Hours in Advance

Network	S_C	P_C	BA	$F1_C$
CNN	0.301	0.397	0.649	0.342
Linear	0.311	0.550	0.526	0.397
LSTM-FCN	0.391	0.694	0.695	0.500
LSTM	0.324	0.588	0.662	0.418
Deep CNN_{skip}	0.283	0.708	0.641	0.4040

As shown in the figure, the model was able to achieve very good forecasting accuracy at the 8-hour time horizon for forecasting, although the forecasting accuracy declined during the 8-hour forecast tests. The source of the geomagnetic disruption from the CME impacting Earth takes some time to manifest. A more or less gradual recovery phase follows the storm's main phase, bringing the Earth's magnetosphere back to balance [20]. Thus, predictive models are not able to extrapolate their forecasts too far into the recovery stage, even into the pre-storm equilibrium state. For this reason, the accuracy of model forecasts declined.

Using Neural Networks has obvious advantages. The application of ML makes the data processing more comprehensive; the model can predict the future eruption of any CME-induced disturbance in real time. Warning hours in advance of major events that could be harmful to the planet and human activities. At the same time, the accuracy of the prediction hours before the geomagnetic burst is guaranteed. The model has a lot of room for development, such as, extending the analysis including forecasting the severity of geomagnetic storm [21] by using a category classification technique and

further revealing the distinctive timescales of the Sun-Earth interactions may further improve the accuracy of geomagnetic storm prediction.

4.3. Very Low Frequency Signal (VLF)

One of the forecasting methods introduced in the end of this chapter is to use very low frequency signal (VLF) to forecast geomagnetic storms. The principle of prediction is that the VLF signal has the characteristics of stability, weak attenuation, and sensitive phase to the external environment. When the solar flare breaks out, the X-ray with sudden increase in flow reaches the ionosphere first with the speed of light, which makes the ionosphere ionization degree deepen, the ionospheric electron density increase, and the equivalent height decrease, which will cause the phase advance of very low frequency signal. Slower high-energy particles take 1-3 days to reach the Earth, causing perturbations in the Earth's magnetic field. Therefore, geomagnetic storms can be predicted by monitoring the phase of very low frequency signals. A large number of data detection results show that the larger the VLF signal phase lead value, the higher the level of solar flares, the greater the likelihood that geomagnetic storms may develop. By inverting the level of a solar flare, one can predict whether a geomagnetic storm is likely to occur one to three days in advance [4].

Solar flares are violent bursts of energy in the sun's atmosphere that cause local gas temperatures to rise momentarily and electrons, protons, and heavy ions to speed up on a roughly 11-year cycle. When the flare bursts out, it radiates huge energy, equivalent to the explosion of tens of billions of million tons of TNT equivalent hydrogen bombs, during which it can be observed that some areas of the solar surface suddenly brighten, and accompanied by the eruption of solar flares radiates electromagnetic radiation such as X-rays, ultraviolet rays, gamma rays, high-energy particle flows, among which the most important is the increase or decrease of X-ray flow, which can increase by 2 to 3 orders of magnitude. The sudden increase in X-rays is the first to reach Earth at the speed of light in a few minutes, while the stream of high-energy particles takes one to three days to reach Earth due to its slower speed. Classification of solar flares: Following the study and observation of space X-rays, scholars decided to classify solar flares into five classes based on the amount of soft X-ray flux measured near the Earth in the 0.1-0.8nm band. Among them, class A and class B flares have a very small impact on the Earth, which is almost negligible, class C is a medium-sized solar flare, which generally has little impact, and class M and flares are relatively large flares, which will have a serious impact on the Earth. Class X is the largest type of flare, and its effects are more severe. The short-term prediction of geomagnetic storms is mainly based on the level of solar flares, which are classified according to the values listed in the Table 3.

Table 3. Classification of solar flares

soft x-ray traffic orders of magnitude $(\mathrm{erg/cm^2 s})$	rank
$\mathrm{Fx} < 10^{-4}$	A
$10^{-4} \leqq \mathrm{Fx} < 10^{-3}$	B
$10^{-3} \leqq \mathrm{Fx} < 10^{-2}$	C
$10^{-2} \leqq \mathrm{Fx} < 10^{-1}$	D
$\mathrm{Fx} \geqq 10^{-1}$	E

The ionosphere is an electrified portion of the Earth's atmosphere, and its fundamental properties are defined by factors such as electron and ion density and temperature. Because the electron density of the ionosphere in the vertical height distribution is very different, Therefore, the distribution of electron density under various height circumstances is the major focus of ionosphere research. The term "electron density" refers to the quantity of electrons present in a unit volume. The atmosphere's density and the sun's radiation intensity change with height, so the electron density varies with the height. Ionospheric electron density distribution with height is shown in Fig. 6 [22].

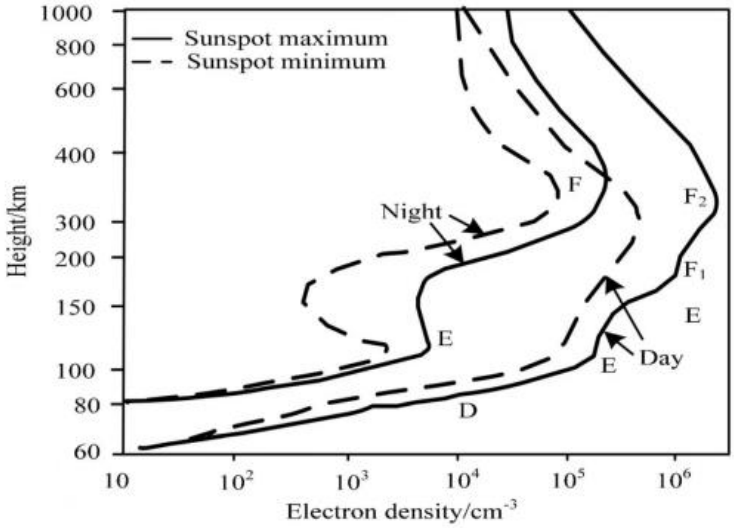


Figure 6. Vertical ionospheric electron density profile

The electron density is affected by the height. The ionosphere is separated into the D layer, E layer, and F layer according to this feature, and the F layer is further divided into the F1 layer and F2 layer. The characteristics of each layer are not introduced in detail in this paper. The total electron content (TEC) of the ionosphere during a flare is significantly higher than usual. VLF is a very low frequency radio wave refers to the frequency of 3-30kHz, wavelength of 10~100km band signal, with stability, weak attenuation and other advantages. During the eruption of solar flares, the phase anomaly of VLF signal is related to the low ionospheric reflection height, operating frequency, propagation path direction, path great circle distance, ground conductivity and other factors. When the propagation path and operating frequency are chosen, the phase anomaly of the VLF signal is determined by the equivalent ionosphere reflection height, which is highly related to the X-ray flow.

Solar flares emit a large number of particles and energy, with the most significant changes in the amount of 1 to 8 angstroms of X-ray, when the flow is thousands of times higher than when the sun is stable. The X-ray radiation emitted by the sun is absorbed by the ionosphere, which greatly promotes the ionization degree of the ionosphere, and the electron density increases, decreasing the equivalent height of the ionosphere and, thus, having an impact on the phase anomaly of the extremely low frequency signal's transmission [23]. On this basis, one can deduce the scale of the solar flare, and then determine whether a geomagnetic storm will occur.

The above is the introduction of the basic knowledge and principles of VLF prediction of geomagnetic storms. In practical applications, it is also necessary to deduce the correlation between the equivalent height of the ionosphere and the X-ray flow rate. In Research on VLF approach for geomagnetic storm prediction, the relationship between the phase change of the VLF signal and the change in ionospheric equivalent height is introduced [4], which will not be repeated in this paper. This method has been successfully applied in practice. Using this method, a VLF receiver is used in Xinxiang, China, to receive signals in three frequency bands sent by Alpha navigation system. The signals are 11.9kHz at Krasnodar's West station, 12.6kHz at Novosibirsk's main station and 14.9kHz at Khabarovsk's East Station [4], The phase data of the very low frequency signals from March 29, 2001 and April 3, 2001 were processed, the magnitudes of the solar flares on those two days were reconstructed according to the fitting equations, and compared with the magnitudes of the solar flares observed on the GOES satellite. On March 31, the Earth's magnetic field received a strong disturbance, and on April 4 and 5, a large geomagnetic storm occurred, which also proved the feasibility of the prediction method. This method also has a lot of room for development, some solar activities generated by the radiation is not in the direction of the Earth, will not have an impact on the earth, for such solar activities, only the very low frequency method to forecast will have a certain false positive rate. Therefore, it is necessary to further study the correlation between VLF signals and geomagnetic storms in order to improve the accuracy and rate of prediction.

5. Conclusion

In the past thousands of years, human footprints have been from the land to the sea, flying into the vast blue sky, but the road of human rope has not stopped, is understanding and studying the broader universe. The space environment has an important impact on spacecraft, communication and navigation, power supply systems, oil pipelines and military activities. Therefore, it is important to study various phenomena in the universe, the physical processes and laws that occur, to predict the occurrence of events, and to slow down or prevent the impact on human activities. Geomagnetic storm is an important phenomenon in space weather and an important object in the study of Sun-Earth relationship. The study of the interplanetary origin and development of geomagnetic storms, their relationship with other space environments, and their impact on human production and life is still one of the important research hotspots at present. The occurrence of geomagnetic storm will bring serious damage to space-based and ground-based technical systems and have a great impact on human living environment, so it is of great practical significance to master the prediction method of geomagnetic storm for improving the forecasting ability of space weather.

Since ancient times, numerous scholars have made great efforts in the study of geomagnetic storms and achieved rich research results. The study of geomagnetic storms can help us better understand the nature of the space environment and the relationship between the sun and the Earth, and also has positive significance to promote the development of other related astrophysical fields. Based on the data collected from geomagnetic storms, this paper systematically introduces the basic concepts, classification and hazards of geomagnetic storms, the interplanetary origin of geomagnetic storms and three forecasting methods of geomagnetic storms: Use the change of cosmic ray flux to predict geomagnetic storms, use neural networks to analyze solar wind data to predict geomagnetic storms and use very low frequency signal (VLF) to predict geomagnetic storms. In addition, the physical principles, advantages, application cases, future development prospects and possible improvement directions of these three forecasting methods are also summarized. Due to space limitations, all types of geomagnetic storms and all possible origins of geomagnetic storms are not described in this paper and there are many geomagnetic storm forecasting methods with different advantages that are not mentioned. In order to further improve the lead and accuracy of geomagnetic storm forecast in the future, it will be a good research direction to explore the combination of a variety of mature forecast methods.

References

[1] Gonzalez W D, Joselyn J A, Kamide Y, et al. What is a geomagnetic storm. Journal of Geophysical Research: Space Physics, 1994, 99 (A4): 5771 - 5792.

[2] Zhu X, Xue B, Cheng G, et al. Application of cosmic ray wavelet analysis to geomagnetic storm prediction. Chinese Journal of Geophysics, 2015, 58 (7): 2242 - 2249.

[3] Telloni D, Schiavo M L, Magli E, et al. Prediction Capability of Geomagnetic Events from Solar Wind Data Using Neural Networks. The Astrophysical Journal, 2023, 952 (2): 111.

[4] Li D. Research on VLF method for geomagnetic storm prediction. Henan Normal University, 2015.

[5] Rostoker G. Geomagnetic indices. Reviews of Geophysics, 1972, 10 (4): 935 - 950.

[6] surutani B T. Solar/interplanetary plasma phenomena causing geomagnetic activity at Earth. Plasmas in the Universe. IOS Press, 2000: 273 - 286.

[7] Richardson I G, Zhang J. Multiple-step geomagnetic storms and their interplanetary drivers. Geophysical research letters, 2008, 35 (6).

[8] Kamide Y, Yokoyama N, Gonzalez W, et al. Two-step development of geomagnetic storms. Journal of Geophysical Research: Space Physics, 1998, 103(A4): 6917-6921.

[9] Dungey J W. Interplanetary magnetic field and the auroral zones. Physical Review Letters, 1961, 6 (2): 47.

[10] Gonzalez W D, Tsurutani B T, Gonzalez A L C, et al. Solar wind-magnetosphere coupling during intense magnetic storms (1978-1979). Journal of Geophysical Research: Space Physics, 1989, 94 (A7): 8835 - 8851.

[11] Kozyra J U, Jordanova V K, Home R B, et al. Modeling of the contribution of electromagnetic ion cyclotron (EMIC) waves to stormtime ring current erosion. Washington DC American Geophysical Union Geophysical Monograph Series, 1997, 98: 187 - 202.

[12] Tong Y. Study on the influence of interplanetary disturbance on the development of geomagnetic storms. Graduate School of Chinese Academy of Sciences (Center for Space Science and Applied Research), 2009.

[13] Echer E, Gonzalez W D, Tsurutani B T, et al. Interplanetary conditions causing intense geomagnetic storms (Dst≤− 100 nT) during solar cycle 23 (1996–2006). Journal of Geophysical Research: Space Physics, 2008, 113: A5.

[14] Echer E, Gonzalez W D, Tsurutani B T. Interplanetary conditions leading to superintense geomagnetic storms (Dst≤− 250 nT) during solar cycle 23. Geophysical Research Letters, 2008, 35 (6).

[15] Zhang J, Richardson I G, Webb D F, et al. Solar and interplanetary sources of major geomagnetic storms (Dst≤− 100 nT) during 1996–2005. Journal of Geophysical Research: Space Physics, 2007, 112: A10.

[16] Wu C C, Lepping R P. Effects of magnetic clouds on the occurrence of geomagnetic storms: The first 4 years of Wind. Journal of Geophysical Research: Space Physics, 2002, 107 (A10): SMP 19-1-SMP 19 - 8.

[17] Wang Y M, Zhang B, Guo L X, et al. Cross Wavelet Analysis and R/S Analysis of Geomagnetic Ap Index and Sunspot number. Scientia Geographica Sinica, 2011, 31 (6): 747 - 752.

[18] King J H, Papitashvili N E. Solar wind spatial scales in and comparisons of hourly Wind and ACE plasma and magnetic field data. Journal of Geophysical Research: Space Physics, 2005, 110 (A2).

[19] Telloni D, Antonucci E, Bemporad A, et al. Detection of coronal mass ejections at L1 and forecast of their geoeffective Ness. The Astrophysical Journal, 2019, 885 (2): 120.

[20] Telloni D, D'Amicis R, Bruno R, et al. Alfvénicity-related long recovery phases of geomagnetic storms: a space weather perspective. The Astrophysical Journal, 2021, 916 (2): 64.

[21] Cander L R, Mihajlovic S J. Forecasting ionospheric structure during the great geomagnetic storms. Journal of Geophysical Research: Space Physics, 1998, 103 (A1): 391 - 398.

[22] Ma Baoke. Research on the influence of ionosphere on radio wave propagation. Xi 'an: Xidian University, 2013.

[23] Zhang Gongliang. Heliospheric and geomagnetic disturbances caused by solar flares. Science in China Series A, 1984.